

Surface conductivity of insulators: two-dimensional cylindrical symmetry

This article has been downloaded from IOPscience. Please scroll down to see the full text article.

2007 J. Phys.: Condens. Matter 19 016002

(<http://iopscience.iop.org/0953-8984/19/1/016002>)

View [the table of contents for this issue](#), or go to the [journal homepage](#) for more

Download details:

IP Address: 129.252.86.83

The article was downloaded on 28/05/2010 at 15:02

Please note that [terms and conditions apply](#).

Surface conductivity of insulators: two-dimensional cylindrical symmetry

S R Holcombe¹, J Liesegang^{1,3} and E R Smith²

¹ Department of Physics, La Trobe University, VIC 3086, Australia

² Department of Mathematics, La Trobe University, VIC 3086, Australia

E-mail: J.Liesegang@latrobe.edu.au

Received 7 June 2006, in final form 20 October 2006

Published 7 December 2006

Online at stacks.iop.org/JPhysCM/19/016002

Abstract

Using results from the derivation of the equations governing surface carrier diffusion of an insulator obtained in Holcombe *et al* (2004 *J. Phys.: Condens. Matter* **16** 5999–6015), an axially symmetric cylindrical system is analysed. Several initial value problems are investigated for a charged flat disc with a grounded circumference in a grounded cylindrical chamber and analytic solutions describing the surface carrier diffusion in the surface region of the disc are obtained. These results are then compared against experimental and numerical results presented in an earlier paper (Soliman *et al* 2005 *J. Phys.: Condens. Matter* **17** 599–617).

1. Introduction

Recent techniques for measuring charge dynamics in polymer materials have included the use of a scanning electron microscope, which delivers a *non-penetrating* electron beam, and a time-resolved current measuring mechanism [1–8]. The effects of charge accumulation are monitored via a measured current as the sample is irradiated (and so charged) until the accumulated charge reaches an asymptotic steady state.

A similar but alternative approach to resistivity measurement [9, 10] involves a sample first being charged and then a portion of its geometry being grounded. The sample is placed in a capacitor arrangement and charge dissipation is measured via capacitive coupling. A recently modified technique [11, 12] based on that used in [9, 10] has a disc-shaped sample irradiated by an electron gun (500 eV) under vacuum. The sample charges via the secondary emission of electrons from its surface. The sample's circumference is then grounded and carrier diffusion measured similarly via the induced charge in a capacitor-like arrangement. The geometry of this new vacuum-based approach differs from that of the previous atmospheric measurements [9, 10] and hence the equations and solutions describing the system must be re-examined.

³ Author to whom any correspondence should be addressed.

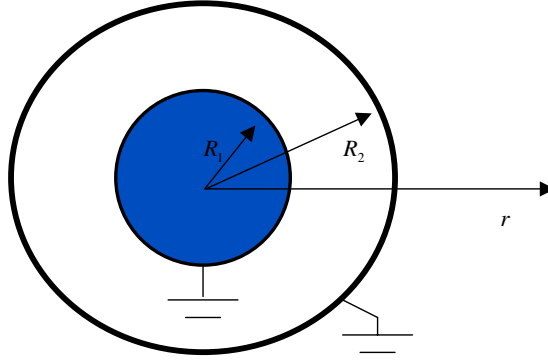


Figure 1. Schematic plan view showing the top of the grounded sample ($r = R_1$) and the vacuum chamber ($r = R_2$) radius (not to scale).

(This figure is in colour only in the electronic version)

In this paper the equations describing the charge carrier diffusion on a sample surface in a coordinate independent form, as derived in [1], are cast into cylindrical coordinates. We show that the charge decay for a simplified two-dimensional axially symmetric system reduces to that of the inviscid Burgers equation [13]. This equation is then solved, with appropriate cylindrical boundary conditions, using both previous methods and the results obtained in [1]. Analytic solutions are obtained for various initial carrier distributions.

2. Cylindrical carrier diffusion

The new resistivity measurement technique described in [11] is essentially based on the same principles and models as defined in [9], the main difference being the charging mechanism. In [9] the samples were frictionally charged under atmospheric conditions. In the new technique the samples are irradiated with electrons under vacuum. The irradiated sample is charged by secondary emission of electrons from its surface, thus leaving a thin layer of ions. The samples are thin discs that, once charged, have their outer circumference ($r = R_1$) grounded, allowing for the carrier diffusion to proceed. The external chamber is also grounded to dissipate any stray charge. This configuration is most easily described via cylindrical coordinates (r, θ, z) and is summarized in figure 1.

In this system, as for the Cartesian system, we assume that the penetration depth of ionic charge in the surface of the sample is small, thus effectively eliminating any dependence on z in the carrier density. We also note that axial symmetry may reasonably be assumed, as we will be dealing with carrier distributions that initially are considered not to depend on the angular coordinate θ . This explicitly means that $n(r, \theta, z, t) \rightarrow n(r, t)$, where $n(r, t)$ is the charge carrier number density.

From this consideration, we choose to simplify the system effectively to one dimension, governed, however, by a two-dimensional axially symmetric boundary condition, and thus from [1] the equations describing the carrier diffusion in cylindrical coordinates become

$$E(r, t) = -\frac{\partial}{\partial r}\phi(r, t) \quad (2.1)$$

$$\frac{1}{r} \frac{\partial}{\partial r} \left(r \frac{\partial \phi(r, t)}{\partial r} \right) = -\alpha n(r, t) \quad (2.2)$$

$$\frac{1}{r} \frac{\partial}{\partial r} (rJ(r, t)) = -q \frac{\partial n(r, t)}{\partial t} \tag{2.3}$$

where E , the electric field, is described via the gradient of a potential function (2.1), which in turn satisfies Poisson’s equation (2.2), and where (2.3) is the equation of continuity. The local charge density in the surface region of the disc at radius r and time t is defined as the product of a carrier density $n(r, t)$ and the charge q of an individual carrier; $\alpha = q/\varepsilon\varepsilon_0$, with ε the sample dielectric constant and ε_0 the permittivity of free space. Charge diffusion in the surface region is assumed to satisfy the continuity condition of (2.3), where the current density is given by $J(r, t)$, which must also satisfy Ohm’s law; namely

$$J(r, t) = q\mu n(r, t)E(r, t).$$

It may be noted that the non-uniformity of the carrier concentration $n(r, t)$ here introduces nonlinearity into this relationship.

The carrier mobility μ is defined via the Einstein–Nernst equation [1] and is given by $\mu = \frac{qD}{kT_0}$, where D is the diffusion coefficient, k is Boltzmann’s constant and T_0 is the temperature in kelvin.

From [1] we also have the time dependence of the electric field, governed via $\nabla \cdot (\frac{\partial}{\partial t} \mathbf{E} + \mu \mathbf{E}(\nabla \cdot \mathbf{E})) = 0$; hence for our cylindrical system we obtain

$$\frac{1}{r} \frac{\partial}{\partial r} \left(r \left(\frac{\partial}{\partial t} E + \mu E \frac{1}{r} \frac{\partial}{\partial r} (rE) \right) \right) = 0. \tag{2.4}$$

(Alternatively, this equation may be briefly derived from equations (2.1)–(2.3) and Ohm’s Law as follows:

From equation (2.3) and Ohm’s Law expressed above, we obtain

$$\mu \frac{1}{r} \frac{\partial}{\partial r} (r n(r, t)E(r, t)) = -\frac{\partial n(r, t)}{\partial t};$$

but equations (2.1) and (2.2) combined yield $\frac{1}{r} \frac{\partial}{\partial r} (rE) = \alpha n(r, t)$ and, using this in the equation immediately above, it follows (by substituting for $n(r, t)$) that

$$\frac{1}{r} \frac{\partial}{\partial r} \left(\mu \frac{\partial}{\partial r} (rE)E + r \frac{\partial}{\partial t} (E) \right) = 0$$

which is equation (2.4).

Integration of (2.4) gives

$$\frac{\partial}{\partial t} E + \mu E \frac{1}{r} \frac{\partial}{\partial r} (rE) = \frac{F(t)}{r} \tag{2.5}$$

where $F(t)$ is an arbitrary function yet to be determined via boundary conditions.

Defining

$$\begin{aligned} E(x, t) &= \frac{\alpha n_0}{r} e(\xi, T), & J(x, t) &= \frac{1}{\sqrt{2}} q\alpha\mu n_0^2 j(\xi, T), \\ \phi(x, t) &= \frac{1}{2}\alpha n_0 \varphi(\xi, T) & \text{and} & & n_0 &= n(r, 0) & \text{at } t = 0 \end{aligned} \tag{2.6}$$

where

$$\xi = \frac{1}{2}r^2, \quad t = \frac{T}{\mu n_0 \alpha} \quad \text{and} \quad n(r, t) = n_0 N(\xi, T) \tag{2.7}$$

with $\int_0^{R_1} N(s, 0) ds = 1$, we obtain the transformed equations of (2.1)–(2.3), (2.5) respectively:

$$e(\xi, T) = -\xi \frac{\partial \varphi(\xi, T)}{\partial \xi} \tag{2.8}$$

$$\frac{\partial}{\partial \xi} \left(\xi \frac{\partial \varphi(\xi, T)}{\partial \xi} \right) = -N(\xi, T) \quad (2.9)$$

$$\frac{\partial}{\partial \xi} \left(\sqrt{\xi} j(\xi, T) \right) = -\frac{\partial N(\xi, T)}{\partial T} \quad (2.10)$$

$$\frac{\partial e(\xi, T)}{\partial t} + e(\xi, T) \frac{\partial e(\xi, T)}{\partial r} = \omega''(T) \quad (2.11)$$

where, as for the Cartesian system [1], the arbitrary function in (2.11) is scaled and written in terms of a second derivative. We also only consider the branch where the inverse of the spatial transformation in (2.7) is positive; i.e. only positive, physical r values are considered.

The electric field driving the diffusion process is related to the current density via Ohm's law, $J = q\mu nE$, which via the above transforms may be expressed as

$$j(\xi, T) = \frac{e(\xi, T)N(\xi, T)}{\sqrt{\xi}}. \quad (2.12)$$

Noting the fact that both the circumference of the sample and the chamber are grounded for $t > 0$, then $\phi(R_1, t) = \phi(R_2, t) = 0$, which from (2.6) and (2.7) implies the transformed boundary conditions of

$$\varphi(\xi_1, t) = \varphi(\xi_2, t) = 0 \quad (2.13)$$

where $\xi_1 = \frac{R_1^2}{2}$ and $\xi_2 = \frac{R_2^2}{2}$ are the transformed radii of the sample and chamber, respectively. In addition to these boundary conditions, it may be seen from (2.8) that

$$e(0, T) = 0 \quad (2.14)$$

which is a result of the angular symmetry imposed on the model, as the potential function satisfying the Poisson equation of (2.2) must satisfy $\frac{\partial \phi}{\partial r}|_{r=0} = 0$ for all time t in order for the function to be defined and bounded on the domain of the sample (otherwise singularities appear in the electric field at the origin).

Equation (2.11) is the same as previously derived for the Cartesian system analysed in [1] and hence many of the methods of solution pertaining to that system apply here.

3. Constant initial carrier density

Considering the case of a constant initial carrier distribution, we have the following initial conditions for the carrier density:

$$N(\xi, 0) = \begin{cases} 1 & 0 \leq \xi \leq \xi_1 \\ 0 & \xi_1 < \xi \leq \xi_2. \end{cases} \quad (3.1)$$

Integrating the transformed Poisson equation of (2.9) for the initial condition above, we have

$$\varphi_{<}(\xi, 0) = -\xi + A \ln(\xi) + B;$$

here A and B are constants of integration and the subscript on the transformed potential indicates that this is a potential defined only for the domain of the sample. Applying the boundary condition of (2.13) for the circumference of the sample, and noting that the potential must be everywhere defined on the sample, then

$$\varphi_{<}(\xi, 0) = \xi_1 - \xi; \quad (3.2)$$

and so the initial electric field on the sample is given from (2.8) as

$$e_{<}(\xi, 0) \equiv g(\xi) = \xi. \quad (3.3)$$

Off the sample, in the annular space containing no carriers, the potential satisfies, from (3.1) and (2.9),

$$\frac{\partial}{\partial \xi} \left(\xi \frac{\partial \varphi_{>}(\xi, T)}{\partial \xi} \right) = 0 \quad \text{for all scaled time } T.$$

Solving this, we have, for the potential off the sample satisfying the condition,

$$\varphi_{>}(\xi_1, T) = 0 \quad \text{and} \quad \varphi_{>}(\xi, T) = c(T) \ln \left(\frac{\xi}{\xi_1} \right)$$

where $c(T)$ is a function chosen so that the potential is continuous for all time T over the boundary of the samples circumference. The potential off the sample, however, must also satisfy the other boundary condition of $\varphi_{>}(\xi_2, T) = 0$, which implies that $c(T) = 0$ is the only solution which satisfies both conditions. Hence

$$\varphi_{>}(\xi, T) = 0 \quad \text{for } \xi_1 < \xi \leq \xi_2 \tag{3.4}$$

and thus, from (2.8),

$$e_{>}(\xi, T) = e_{>}(\xi_1+, T) = 0 \quad \text{for } \xi_1 < \xi \leq \xi_2. \tag{3.5}$$

The time evolution of the electric field on the sample is such that it must satisfy (2.11), thus from the prior analysis [1] via the method of characteristics we have the time evolution of the field on the sample given by

$$e(\xi, T) = g(\eta(\xi, T)) + \Omega'(T) \tag{3.6}$$

where

$$\eta(\xi, T) = \xi - Tg(\eta(\xi, T)) - \Omega(T) \tag{3.7}$$

and

$$\Omega(T) = (\omega(T) - \omega(0) - T\omega'(0)). \tag{3.8}$$

Solving for η in (3.7) using (3.3) and then substituting back into (3.6) gives the electric field on the sample as

$$e(\xi, T) = \frac{\xi - \Omega(T)}{T + 1} + \Omega'(T). \tag{3.9}$$

From the boundary condition of (2.14) we must have

$$\Omega'(T) - \frac{\Omega(T)}{T + 1} = 0. \tag{3.10}$$

Solving this differential equation, we have $\Omega(T) = (T + 1)B$, where B is a constant. From (3.8), however, we note that $\Omega(0) = 0$, hence $B = 0$, and therefore it is established that

$$\Omega(T) = 0 \quad \forall T. \tag{3.11}$$

Equation (3.9) then becomes

$$e(\xi, T) = \frac{\xi}{T + 1}. \tag{3.12}$$

From (2.9) and (2.12), the normalized carrier density and current density may be obtained as:

$$N(\xi, T) = \frac{1}{T + 1}, \quad \text{and} \quad j = \frac{\sqrt{\xi}}{(T + 1)^2}. \tag{3.13}$$

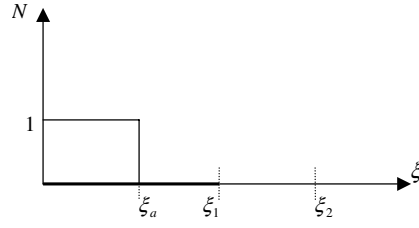


Figure 2. Schematic diagram depicting the carrier distribution in relation to the transformed sample radius ξ_1 and chamber radius ξ_2 .

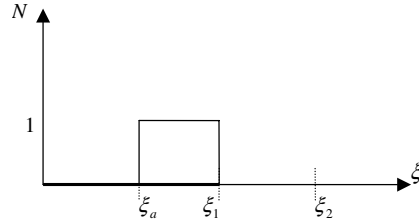


Figure 3. Schematic diagram depicting the carrier distribution in relation to the transformed sample radius ξ_1 and chamber radius ξ_2 .

It may be noted that the carrier density is of the same form as that obtained for the Cartesian system and that the above satisfy the continuity condition in (2.10); i.e.

$$\frac{\partial}{\partial \xi} (\sqrt{\xi} j) = \frac{1}{(T + 1)^2} = -\frac{\partial N}{\partial T}.$$

Inverting the transformed variables, we obtain the true form of the carrier density in hyperbolic form as

$$n(r, t) = \frac{n_0}{\mu \alpha n_0 t + 1}. \tag{3.14}$$

4. Discontinuous constant carrier distributions on the sample

We now consider two additional cases (see figures 2 and 3), namely that of a carrier distribution defined by

(i)

$$N(\xi, 0) = \begin{cases} 1 & 0 \leq \xi \leq \xi_a \\ 0 & \xi_a < \xi \leq \xi_2 \end{cases} \quad \xi_a < \xi_1 \tag{4.1}$$

and

(ii)

$$N(\xi, 0) = \begin{cases} 0 & 0 \leq \xi < \xi_a \\ 1 & \xi_a \leq \xi \leq \xi_1 \\ 0 & \xi_1 \leq \xi \leq \xi_2 \end{cases} \quad \xi_a < \xi_1. \tag{4.2}$$

In either case it may be seen, as was shown previously, that the potential and the electric field on the domain of $\xi_1 < \xi \leq \xi_2$ is zero, and will not be considered in what follows.

For the first case (i) the initial potential function is determined by integrating (2.9)

$$\varphi_{<}(\xi, 0) = A - \xi \tag{4.3}$$

where there is no constant to ensure that the function is defined at the origin, and the subscript on the potential function indicates that the domain is one in which carriers are defined. In the region on the sample absent of carriers, the potential is

$$\varphi_{>}(\xi, T) = B(T) \ln\left(\frac{\xi}{\xi_1}\right). \quad (4.4)$$

For the potential to be continuous and smooth over the boundary where carriers are defined, each potential must have the same value and gradient at that point, which allows for solution for the unknowns. Note from (4.3) that this is the same situation as for the full constant carrier example, and hence from (3.12) the electric field for the charged area is

$$e_{<}(\xi, T) = \frac{\xi}{T+1}. \quad (4.5)$$

From the method of characteristics and (3.7), namely

$$\xi(0) = \xi(T) - Tg(\xi(0)) \quad (4.6)$$

where it has already been shown that $\Omega(T) = 0$, any point lying on the characteristic that solves the equation must satisfy (4.6). Therefore, focusing on the boundary of the charged area (i.e. $\xi(0) = \xi_a$) and solving (4.6), the time evolution for that boundary from its initial point ξ_a is

$$\xi(T) = (T+1)\xi_a \quad (4.7)$$

since, for the charged area on the sample, $g(\xi) = \xi$. From (4.7), where the right-hand side is a function of T , it may be seen that the boundary is moving linearly with respect to time, and so the question may now be asked as to which direction the boundary is moving by assuming various points on the domain for $\xi(T)$.

First assume that the boundary moves slightly from its initial position towards the origin; one obtains:

$$(T+1)\xi_a = \xi_a - \Delta\xi \quad \text{such that } \Delta\xi_a > 0;$$

therefore the time it has taken to move $\Delta\xi$ from the initial boundary point is $T = -\frac{\Delta\xi}{\xi}$ and, since ξ is always positive, we have a time that is negative, which indicates that this position must have been occupied in the past. It follows that the boundary must be moving towards the edge of the sample; therefore, setting $\xi(T) = \xi_1$ and solving (4.7) for T :

$$T_c = \frac{\xi_1 - \xi_a}{\xi_a}. \quad (4.8)$$

The subscript is explicitly included to remind us that this is the time it takes for the boundary of the charged area to diffuse to the edge of the sample, after which the system then becomes that of the constant initial carrier density as studied in section 3. The carrier density may be obtained from (4.5) as

$$N(\xi, T) = \frac{1}{T+1}; \quad (4.9)$$

therefore at the change over time of (4.8) where the system becomes that as described in section 3:

$$N(\xi, T_c) = \frac{\xi_a}{\xi_1}. \quad (4.10)$$

Inverting this to obtain the true carrier density:

$$n(r, t_c) = n_0 \frac{R_a^2}{R_1^2} \equiv \bar{n}_0. \quad (4.11)$$

Note that this is the initial density for the case of constant carrier distribution over the entire sample defined as \bar{n}_0 , where the magnitude of the density is reduced by the ratio of the area of the initial carrier distribution to that of the area of the sample as a whole. Thus the initial discontinuous carrier density diffuses, spreading over the surface of the sample to become distributed over the entire sample, at which time we simply have a constant initial carrier density problem, where the initial density is given by (4.11).

Following a similar approach for the second case (ii):

$$e(\xi, 0) = \xi - \xi_1 \quad \text{on } \xi_a \leq \xi \leq \xi_1 \quad (4.12)$$

where the carrier distribution is defined, and

$$e(\xi, T) = 0 \quad \text{on } 0 \leq \xi \leq \xi_a \quad (4.13)$$

since, by (2.14), $e(0, T) = 0$. From (3.6), and (4.12)

$$\eta = \frac{\xi(T) + T\xi_1}{(T+1)} = \xi(0) \quad (4.14)$$

and hence

$$e(\xi, T) = \frac{\xi - \xi_1}{(T+1)}. \quad (4.15)$$

We again ask in which direction the boundary is moving by first analysing points to the right of the boundary, i.e.

$$\frac{\xi_a + \Delta\xi + T\xi_1}{(T+1)} = \xi_a$$

from which we find

$$T = \frac{\Delta\xi}{(\xi_a - \xi_1)} < 0,$$

since $\xi_a < \xi_1$ by definition, and it is concluded that the boundary is moving to the left toward the origin. Therefore the time at which the boundary meets the origin and the system becomes that of a constant carrier distribution over the entire sample is given by $T_c = \frac{\xi_a}{\xi_1 - \xi_a}$.

The evolution of the carrier density is again found to be $N(\xi, T) = \frac{1}{T+1}$, where the true carrier density at the change-over time is

$$n(r, t_c) = n_0 \frac{R_1^2 - R_a^2}{R_a^2 + 2} \equiv \bar{n}_0$$

and the carrier density is denoted as \bar{n}_0 , representing the initial carrier density for what has now become a continuous and constant distribution of charge over the entire sample.

5. Experimental observations

Observations have been made in [14], using a method by which surface resistivity can be measured from a flat disc-shaped sample charged via a custom-built electron gun in a cylindrical chamber under vacuum. This is an improvement over early methods discussed in [9, 10]. Such techniques in [14], inherent within a cylindrical geometry and with a sample grounded on its circumference, are therefore appropriate for discussion and comparison with the theory outlined here.

In [14], approximate solutions for time $t \ll 1$ are derived and shown to be equivalent in form to those in [9]. The same solution is obtained here as (3.14) whereby, as in [14], we assume initially that the sample is charged with a constant carrier distribution over the

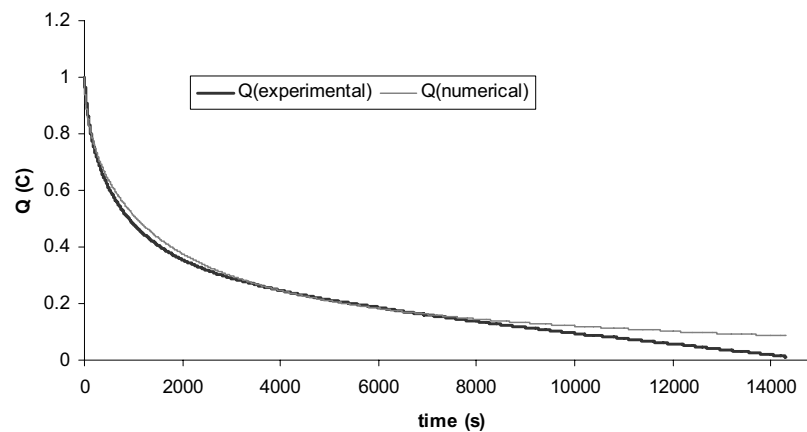


Figure 4. Plot of normalized charge on a glass sample against time: experimental observations compared with the three-dimensional numerical model presented in [14] plotted over an extended period $t \in [0, 143\,00]$ s.

sample's entire surface (section 3). Comparisons against experimental observations are clearly and explicitly discussed in [14] and we will not draw too much attention to them here, other than to say that, for early stages, in the diffusion process the solution (3.14) provides a good approximation and yields values of resistivity that are also in good agreement within established literature. Further, in [14], a numerical solution is provided that encompasses a three-dimensional model of the chamber and sample, and numerical results against experimental data again are in good agreement. It is interesting to note that, in [14], equation (3.14) was derived via approximating the defining differential equations. Here no such approximation occurs and therefore we consider (3.14) to be the exact solution for the two-dimensional cylindrical approximation, given the initial assumptions that (a) such a model is merely an approximation to the experimental system and (b) initial carrier diffusion on the sample can adequately be approximated as being constant over the entire sample. With this in mind, we continue.

What is of main importance here is the discrepancy between the analytic solution of the model (approximating the system in [14]) that can be noted for diffusion processes observed over longer periods of time. Towards this, we provide a normalized plot of experimental data for the glass sample over an extended diffusion period compared to that in [14] (in [14], $t \in [0, 12\,000]$ s). We compare this data against two theoretical models, namely the numerical model presented in [14] which solves the three-dimensional system and the hyperbolic solution presented here (3.14). We choose to fit (3.14) against the experimental data via performing a nonlinear least squares fit. We thus obtain the following.

In figure 5, equation (3.14) was fitted against the normalized experimental data by assuming the general hyperbolic form of

$$n = \frac{1}{At + 1}.$$

This was used in Mathematica with the nonlinear fit function against the entire sample range of experimental data from which the constant A was determined. Meanwhile, given the nature of the derivation of the formulae (3.14) in [14], in which it is stated (under the presumptions used in the derivation) that the validity of the formulae is for initial diffusion periods, here we have used (3.14) over the entire period of diffusion. This is valid, since in our derivation here we indeed have shown that (3.14) (from the initial condition) is valid for the entire diffusion process and not merely the initial stages. One must remember that in [14] we use an approximation on

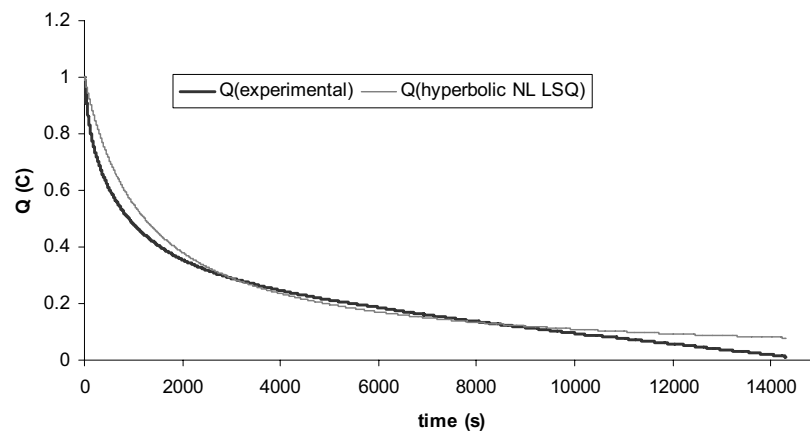


Figure 5. Plot of normalized charge on a glass sample against time: experimental observations compared with the two-dimensional analytic solution (3.14) plotted over an extended period $t \in [0, 14300]$ s.

the differential equation in order to obtain (3.14) and that approximation is only true for small (or possibly large) time t .

From figure 4 we note rather good agreement with experimentally observed data, particularly in the period up until a range within 6000–8000 s in which we observe a definite deviation in the theoretical model away from observed data points.

In figure 5 the difference between the model and experiment is more striking. This is possibly because we are modelling a three-dimensional experiment with a two-dimensional theoretical system. While it is fair that a distinct initial period differs from experiment over all the approximation, note also that there is a deviation in the theoretical model away from the observed data points towards the tail end of the diffusion process. There is in fact a 0.999 correlation factor with experimental data for the glass sample over $t = 6000$ – 14300 s and that of a linear fit. There is no such correlation with the two-dimensional solution (3.14), nor does there appear to be any such correlation with the numerical solution of the three-dimensional model presented in [14]. The fact that the two-dimensional model veers away from the observed experimental plot may be excused, given that it is after all an approximation to a three-dimensional system in which we have admittedly ignored any dependence of the electric field on height, thus also ignoring another boundary condition. The numerical solution and its divergence away from the observed data on the other hand raise questions about the model. It must be remembered however that, even with the three-dimensional numerical solution, we are still approximating the experimental system, in that we are *assuming* that initially all charge is a constant distribution over the sample's surface. This assumption obviously impacts on the very form of solution that we obtain from the system of differential equations. Therefore we must now reconsider either our initial conditions or indeed the possibility that we may model the diffusion process in what is appearing to be two stages: one in which a hyperbolic/nonlinear form of solution is present in the first stage of diffusion and another stage in which the medium begins to diffuse linearly. In order to do this, we must re-examine the theory, and this we leave for another paper.

6. Conclusion

Previously obtained results for a generalized model of surface carrier diffusion in insulators, particularly for a one-dimensional Cartesian system [1], have been applied to a two-

dimensional cylindrical system. It has been shown that the system, as for the Cartesian case, reduces to that of the one-dimensional inviscid Burgers equation. This equation was solved using the method of characteristics and boundary conditions that reflect the experimental design of the vacuum resistivity measurement technique briefly discussed in [1] and examined in [11, 12]. Similar initial conditions as posed in [1] were examined and the dynamics of such conditions analysed. It was observed that, unlike the Cartesian case, the non-homogenous ‘driving’ term of the inviscid Burgers equation vanishes for the given boundary conditions. It was also observed that the carrier density is of the same form as that for the Cartesian case and depicts a hyperbolic decay of charge from the sample’s surface. The hyperbolic solution was compared to experimentally observed data as well as against the three-dimensional numerical solution presented in the largely experimental paper [14], though here we do so over an extended period of diffusion. This comparison mainly presents a divergence of theory from experimental data for the latter period of diffusion in both the two-dimensional model presented in this paper as well as for the three-dimensional numerical solution presented in [14]. This divergence, it is inferred, is possibly the result of an incorrect or over-approximated initial condition. It was also mentioned that there may possibly be two distinct stages of diffusion: one nonlinear and the other linear.

References

- [1] Holcombe S R, Liesegang J and Smith E R 2004 Surface conductivity of insulators: one-dimensional initial value problems and the inviscid Burgers equation *J. Phys.: Condens. Matter* **16** 5999–6015
- [2] Gong H, Song Z G and Ong K C 1997 *J. Phys.: Condens. Matter* **9** 1–5
- [3] Laurenceau P, Dreyfus G and Lewiner J 1977 *Phys. Rev. Lett.* **38** 46
- [4] Gerhard-Multhaupt R 1983 *Phys. Rev. B* **27** 2494
- [5] Cals M P, Marque J P and Alquie C 1992 *IEEE Trans. Electron. Insul.* **27** 763
- [6] Berstein J B and Cooke C M 1991 *IEEE Trans. Electron. Insul.* **26** 1080
- [7] Takada T, Maeno T and Kushibe H 1992 *IEEE Trans. Electron. Insul.* **22** 497
- [8] Liu R S, Takada T and Takasu N 1993 *J. Phys. D: Appl. Phys.* **26** 986
- [9] Liesegang J, Senn B C and Smith E R 1995 Resistivity of static and antistatic insulators from surface charge measurement *J. Appl. Phys.* **77** 5782
- [10] Liesegang J and Senn B C 1996 Resistivity, charge diffusion and charge depth determinations on charged insulator surfaces *J. Appl. Phys.* **80** 6336
- [11] Soliman A 2003 *Doctoral Thesis* La Trobe University Bundoora, Australia
- [12] Holcombe S R 2003 Shockwave theory of surface carrier diffusion in insulators *Doctoral Thesis* La Trobe University Bundoora, Australia
- [13] Burgers J 1948 A mathematical model illustrating the theory of turbulence *Advances in Applied Mechanics* (New York: Academic)
- [14] Soliman A H, Holcombe S R, Pigram P J and Liesegang J 2005 Surface conductivity of insulators: a resistivity measurement technique under vacuum *J. Phys.: Condens. Matter* **17** 599–617